

# Impact of calcium sulfate additions on the hydration of the belite phase in cements made from belite-ye'elimite-ferrite clinkers

V. Morin<sup>1</sup>, I. Baco , P. Termkhajornkit, B. Albert

*Lafarge Research Center, Process & Environment Program, 38291 Saint Quentin Fallavier, France*

## **Abstract**

*“BYF” clinker, mainly composed of belite, ye'elimite and calcium alumino-ferrite, is a low-CO<sub>2</sub> alternative to Portland cement clinker. Simple BYF cements are made by adding calcium sulfate to BYF clinker, typically in amounts larger than normally used in Portland cements. In this work the hydration kinetics of BYF cement pastes made with three different clinkers and three different calcium sulfate contents are studied. A dedicated Rietveld refinement file was developed in order to quantify the phase assemblage formed during hydration. Results show that increasing the ye'elimite/belite ratio in the clinker at constant added calcium sulfate results in greater formation of strätlingite at the expense of C-S-H. Increasing the level of calcium sulfate addition at constant clinker composition results in the formation of more ettringite at very early ages, and thus gives higher early strengths, but this tends to block the onset of belite hydration which can lead to slow strength development at later ages. It is hypothesized that the blockage of belite hydration occurs due to the limited access of water resulting from the deposition of ettringite around belite grains.*

## **Originality**

*Development of a dedicated Rietveld control file and better understanding of belite hydration in Belite-Ye'elimite-Ferrite cements.*

**Keywords:** *Hydration; belite; calcium sulfoaluminate; calcium sulfate*

<sup>1</sup> Corresponding author: [vincent.morin@lafarge.com](mailto:vincent.morin@lafarge.com), Tel +33-474 821 824, Fax ++33-474 168 0 00

## 1. Introduction

BYF cements, based on clinkers comprising mainly belite, ye'elimite and calcium aluminoferrite, have a significant potential to reduce CO<sub>2</sub> emissions per unit of concrete relative to Portland cements (Li *et al.*, 2007). They represent a class of cements intermediate between belite-rich Portland cements and calcium sulfoaluminate (CSA) cements of the type developed in China over 30 years ago (Wang and Su, 1993). BYF clinkers generally require less alumina in their raw materials (e.g. in the form of bauxite) than CSA clinkers, which helps reduce raw materials costs; and, like CSA clinkers, BYF clinkers can be produced in conventional rotary kilns. The low CO<sub>2</sub> emissions arise mainly from the smaller amount of limestone that must be decarbonated per unit of clinker, which also results in a reduced enthalpy of clinker formation (Mehta, 1980; Lea, 1998; Sharp *et al.*, 1999; Gartner, 2004). The reduced clinkering temperature (150-200°C lower than for Portland clinker production) reduces kiln heat losses and typically also results in BYF clinkers that require less energy to grind than Portland clinkers. Finally, calcium sulfates can be added to the cement in greater amounts than in Portland cements, further diluting the clinker with a lower-embodied-CO<sub>2</sub> raw material.

The successful development of BYF cements and their ultimate acceptance for a range of concrete applications requires a deep understanding of their hydration mechanisms, which in turn requires the development of improved analytical techniques. Since many of the hydrates formed are crystalline, quantitative X-Ray diffraction methods are useful. Thus, we have developed dedicated Rietveld control files for quantification of both the clinker phases and the hydrated phases. This paper discusses some specific issues encountered in the development of these Rietveld control files and explains how the Rietveld method has been used to understand the impact of the amount of added calcium sulfate on the rate of hydration of BYF clinkers, and especially of the belite phase in such clinkers.

## 2. Experimental

### 2.1. Raw materials

BYF clinkers were made from mixtures of limestone, clay, bauxite, iron ore and anhydrite, ground together in the desired proportions, pelletized and burned in a rotary kiln or an electric lab furnace at a maximum temperature of around 1300°C. Boron, in the form of colemanite, a natural calcium borate mineral, was added so as to give 1.38% B<sub>2</sub>O<sub>3</sub> on a clinker basis in order to stabilize  $\alpha'$ -C<sub>2</sub>S, which is a more hydraulically reactive phase than the  $\beta$ -C<sub>2</sub>S typically present in Portland cement clinker (Chae W.H., *et al.* 1996, Jelenic I., 1978). This high temperature polymorph can also be stabilized by alkali metals (Gies A., *et al.* 1986) or a mixture of alkali metals and iron (Suzuki K., 1980). For cement preparation, the clinkers were ground alone to the required fineness and ground calcium sulfate was blended with the ground clinker in the desired proportions. Five different cements were studied, based on three different clinkers (A, B and C) with significantly different phase proportions. Three cements (C1, C2 and C3) were made from clinker C with different levels of calcium sulfate addition.

Cement A was based on a high-ye'elimite BYF clinker produced during an industrial trial in France (Burgundy), to which 8% anhydrite and 2% hemihydrate was added. Its Blaine fineness was 420 m<sup>2</sup>/kg. Its estimated mineralogical composition is given in table 1:

Table 1: Cement A composition

Composition %	Ye'elimite	Belite	Ferrite	Gehlenite	Anhydrite	Hemi-hydrate	Other phases
Cement A	31	36	13	1.5	8	2	8.5

Cement B was based on a low ye'elimite laboratory-made BYF clinker to which 10% anhydrite was added. Its Blaine fineness was 400 m<sup>2</sup>/g. Its estimated mineralogical composition is given in table 2:

Table 2: Cement B composition

Composition %	Ye'elimite	Belite	Ferrite	Gehlenite	Anhydrite	Hemi-hydrate	Other phases
Cement B	14	53	21	0	10	0	2

The last three cements were based on a third clinker (C) produced in pilot plant in Poland (RCBM), with three different levels of anhydrite addition. The measured cements composition are given in table 3:

Table 3: Cement C compositions

Composition %	Ye'elimite	Belite	Ferrite	Gehlenite	Anhydrite	Hemi-hydrate	Other phases
Cement C1	28	50	19.6	0	2.4	0	0
Cement C2	27	48	18.8	0	6.2	0	0
Cement C3	24.7	44	17.3	0	14	0	0

The Blaine fineness of cement C1 , C2 and C3 is 400 m<sup>2</sup>/g.

## 2.2. Experimental Process

### 2.2.1 X-Ray powder diffraction measurement

X-ray powder diffraction (XRD) measurements were carried out using CuK $\alpha$  radiation on a PANalytical X'Pert Pro diffractometer in a  $\theta$ -2 $\theta$  configuration with an angular scan 5°-65° (2 $\theta$ ) and an X'Celerator detector.

### 2.2.2 Sample preparation for hydration studies of cement paste

The cement is mixed with water at a water/cement ratio of 0.50 and at 20±1°C. The paste is poured into 40ml plastic containers which are then sealed and stored at 20±1°C. At each chosen age a new plastic container is opened and the paste inside is ground to completely pass a 100 $\mu$ m sieve, after which the powder is dried rapidly to stop further hydration, using the acetone-ether method (Wang J., *et al*, 2010).

### 2.2.3 Clinker phase quantification by the Rietveld refinement method

Conventional ICSD patterns, as shown in Table 4, were used in the Rietveld control file. The brownmillerite type ferrite phase composition is closer to C<sub>6</sub>AF<sub>2</sub> than C<sub>4</sub>AF in BYF cement (Wang J., 2010). Two polymorphs of ye'elimite (cubic and orthorhombic) can co-exist in BYF cement and these phases were already studied by X-Ray powder diffraction (Cuesta, *et al*, 2014).

Table 4 ICSD pattern of main anhydrous cement phases

Cement phases	Common formula	ICSD reference
Ye'elimite ortho.	C <sub>4</sub> A <sub>3</sub> S	80361
Ye'elimite cubic	C <sub>4</sub> A <sub>3</sub> S	9560
Belite (alpha')	C <sub>2</sub> S	81097
Belite (beta)	C <sub>2</sub> S	963
Belite (gamma)	C <sub>2</sub> S	9095
Brownmillerite (ferrite)	C <sub>6</sub> AF <sub>2</sub> (Ca2 (Al0.663, Fe1.337) O5)	98832

### 2.2.4 Hydrate quantification by the Rietveld refinement method

The main hydrated phases detected in BYF cement pastes are ettringite, strätlingite, calcium monosulfoaluminate (with 12 and 14 H<sub>2</sub>O), bayerite and gibbsite (aluminum hydroxide), siliceous hydrogarnets and C-S-H (Morin V., *et al*, 2011). The specific ICSD patterns that were in the Rietveld control file for this study are listed in Table 5:

Table 5 ICSD pattern of main hydrated phases

Cement phases	Common formula	ICSD pattern
Ettringite	C <sub>3</sub> A.3CS.32H	16045
Monosulfoaluminate 12H	C <sub>3</sub> A.CS.12H	100138
Gibbsite	AH <sub>3</sub>	6162
Bayerite	AH <sub>3</sub>	26830
Strätlingite	C <sub>2</sub> ASH <sub>8</sub>	69413
C-S-H (Tobermorite)	C <sub>5</sub> S <sub>6</sub> H <sub>5</sub>	87689

Several remarks about our construction of the Rietveld control file for hydrated phases quantification:

1. A calcium monosulfoaluminate AFm phase with 14 H<sub>2</sub>O is often detected during hydration of BYF cements. For its quantification in our Rietveld control file, we use the ICSD pattern of calcium monosulfoaluminate with 12 H<sub>2</sub>O with a modification of the lattice parameter “c” to fit the basal spacing peaks.
2. We used the external standard method with rutile. The XRD intensity profile of cement paste was mathematically mixed with the XRD intensity profile of rutile with fraction by mass 50: 50 percent. Two main poorly-crystallized or amorphous phases can be formed during BYF hydration: aluminium hydroxide (AH<sub>3</sub> “gel”) and C-S-H. For the former, a specific method of quantification was developed for this study (hkl fitting method) as detailed under “Results and Discussion.” The later was calculated indirectly thanks to the external standard: rutile.
3. Siliceous hydrogarnets with the general formula Ca<sub>3</sub>(Al,Fe)<sub>2</sub>(SiO<sub>4</sub>)<sub>3-y</sub>(OH)<sub>4y</sub> (with y=3-0) are known to form during BYF cement hydration (Wang et al., 2010). Special Rietveld control files were made for this study to improve the accuracy of the quantification and the estimation of the composition of siliceous hydrogarnets, as detailed under “Results and Discussion.”
4. When using the XRD-Rietveld analysis to quantify the phases in hydrated cement pastes, the calculation is done relative to the acetone-ether-dried paste. In order to normalize the phases relative to the initial mass of anhydrous cement, we measure the mass loss at 550°C for each paste sample by TGA, and calculate the phase composition relative to initial cement using the following equation, which assumes that all hydrates are decomposed at 550°C and that the initial cement does not contain significant amounts of hydrated phases:

$$\%_{Anh / Hyd.phase.normalized} = \frac{\%_{Anh / Hyd.Rietveld.phase}}{\left(1 - \left(\frac{\%weightloss.(25 - 550^{\circ}C)}{100}\right)\right)} \quad (1)$$

### 3. Results and Discussion

#### 3.1. Advances in Rietveld control file construction

##### 3.1.1 Quantification of hydrated alumina phases

During BYF hydration, belite reacts initially with hydrated alumina, generically referred to here as “AH<sub>3</sub>,” to give strätlingite (Wang et al., 2010):



The AH<sub>3</sub> itself results from the rapid initial reaction of ye’elinite with calcium sulfate and water, which produces ettringite if excess C\$ is present:



and produces monosulfoaluminate once all of the free C\$ has been consumed:



The resulting hydrated alumina phases can be identified to some extent in the X-ray diffraction scan via broad peaks around 18.2° and 20.5° corresponding to peaks position of gibbsite and bayerite.

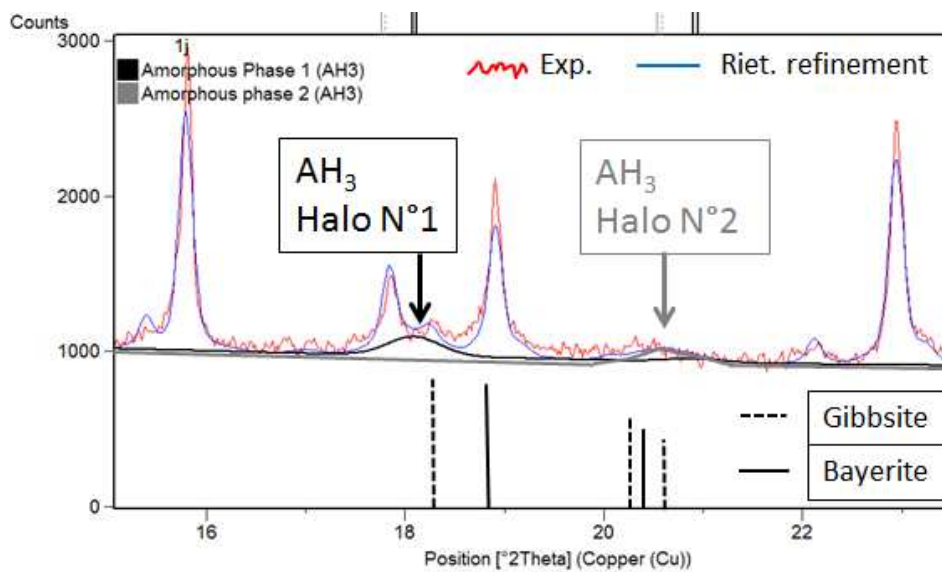


Figure 1: AH<sub>3</sub> peak positions and quantification method

However, if we simply use the ICSD patterns of gibbsite and bayerite in the Rietveld control file, we get poor quantification of the hydrated alumina. In order to improve our quantification of this AH<sub>3</sub>, we created two AH<sub>3</sub> phases in our control file with hkl fitting method: the first phase was focused on the so called “halo N°1” at around 18.2° and the second phase at “halo N°2” at around 20.5°. These two broad peaks were obtained by choosing adequate crystallographic length a, b and c and adjusted with the w parameter (peak width) in order to fit the experimental halo. Finally, the pseudo mass factors corresponding to these two broad peaks were adjusted so that the total amount of gibbsite and bayerite calculated corresponded to the values predicted by equation 3 and 4.

### 3.1.2 Siliceous Hydrogarnet quantification

#### 3.1.2.1 Low-Silicon Hydrogarnet (L-Si-Hg)

When belite hydration starts, strätlingite forms following eq. (2) until  $AH_3$  is exhausted, after which further belite and ferrite hydration produce lime which reacts for instance with strätlingite to give siliceous hydrogarnets of general composition  $(Ca_3(Al,Fe)_2(SiO_4)_{3-y}(OH)_{4y})$  with  $y=0-3$  (Wang et al, 2010). In our XRD scans and at early age, we observe this as a shift of peaks at around  $17.5^\circ$  and  $20.2^\circ$  that initially correspond to  $C_3AH_6$  (ICSD 94631) but shift toward higher angles with hydration time. This shift appears mainly to be due to silicon incorporation into the hydrogarnet, in which one  $Si^{4+}$  replaces  $4H^+$ ; it is consistent with the literature (Dilnesa B.K., 2011) which implies that a continuous solid solution is found at low Si/H ratios. We used the hydrogarnet pattern ICSD 94631 with a suitable  $w$  parameter (peak width) in order to follow the peak shift and get the best possible quantification of this continuous solid solution phase, which we named “Low Silicon Hydrogarnet” (L-Si-Hg).

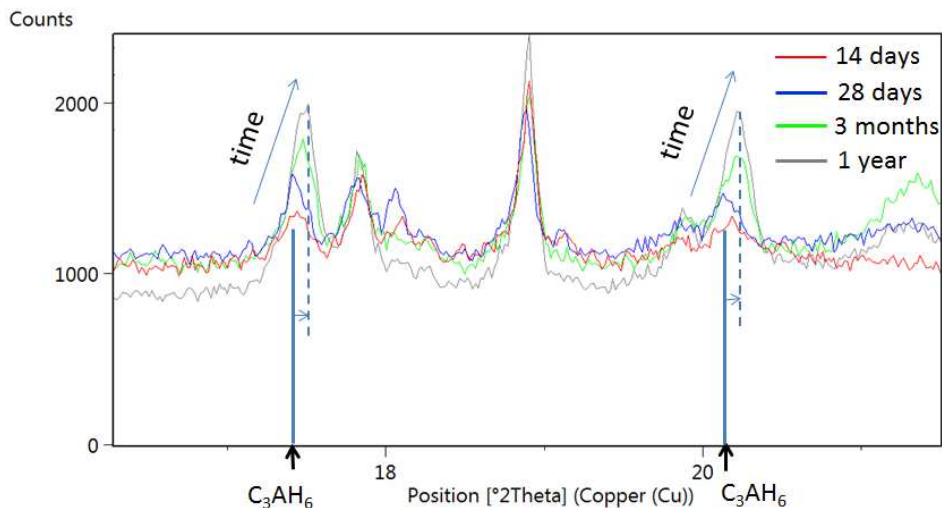


Figure 2: hydrogarnet peak positions and peaks shift as a function of hydration time

#### 3.1.2.2 High-Silicon Hydrogarnet (H-Si-Hg)

At later ages (see Fig. 3) we observe the formation of peaks at  $39.8^\circ$ ,  $45.2^\circ$ ,  $53.5^\circ$  and  $55.7^\circ$  that appear more consistent with a high-silicon hydrogarnet (H-Si-Hg) phase, such as that of ICSD pattern 83715,  $[Ca_3(Al_{0.13},Fe_{0.87})_2(SiO_4)_{1.65}(OH)_{5.4}]$  and this hydrated phase formation is concomitant with a decrease of strätlingite amount. This ICSD pattern allows us to roughly quantify this phase, but it seems unlikely that it actually has such a high iron content, despite the fact that a considerable amount of iron is available from ferrite phase hydration. The peak positions of the ICSD pattern 83715 fit well with XRD scan but the peak intensity at  $55.7^\circ$  is too high, probably due to a lower iron content. The substitution of A for F in  $C_3FSH_6$  shifts these two peaks to higher angles and decreases their intensities (Dilnesa, et al, 2011), while a decrease in the Si/H ratio leads to a shift towards lower angles that can compensate. In Fig. 4. we compare ICSD 83715 (Pattern N°1) with ICSD 31250 (Pattern N°2) of  $Ca_3Al_2Si_{1.53}O_{12}H_{5.88}$ . All the peaks are shifted to higher angles but the peak intensities at around  $28.9^\circ$  and  $55.7^\circ$  of Pattern N°2 seem to match better with the experimental scan. So, based on these two ICSD patterns, a better or more “real” composition for our H-Si-Hg phase can be extrapolated: it should contain more iron and less silicon than the phase of in Pattern N°2. Both of these modifications

will shift the peaks towards lower angles and will lead to better matches with the experimental scan in term of intensity and peaks positions.

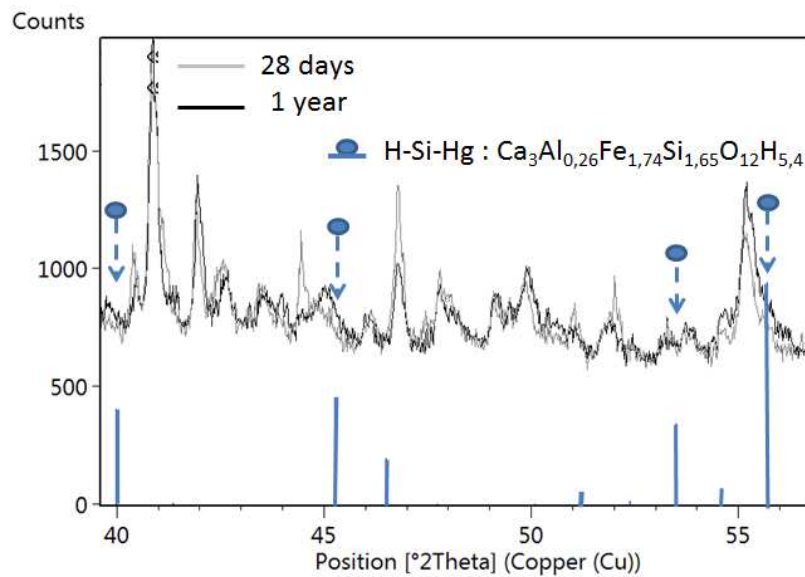


Figure 3 High siliceous-hydrogarnet formation at long hydration times

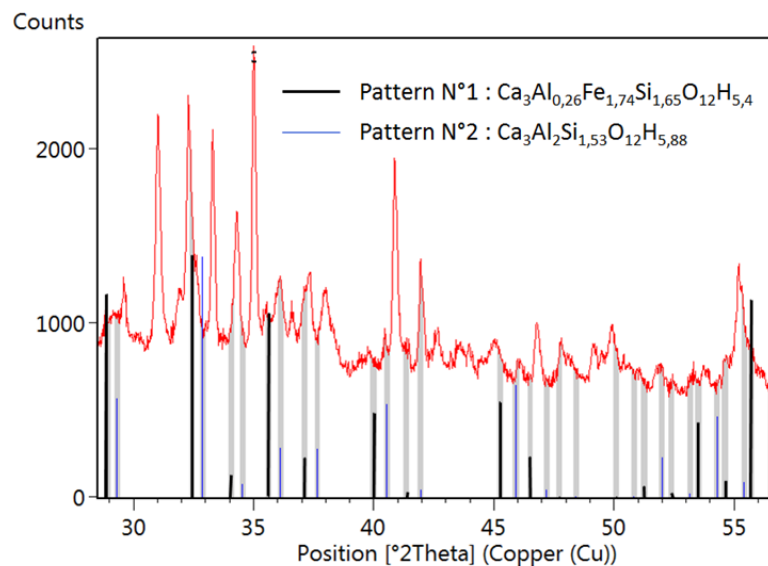


Figure 4 peak positions of two different high siliceous hydrogarnets.

It is worth noting that experimentally these low and high siliceous hydrogarnets can co-exist at long term in BYF cement. Dilnesa, et al. 2011 showed that continuous change of siliceous iron hydrogarnet composition is possible from approximately  $C_3FS_{0,25}H_{5,5}$  to  $C_3FS_{0,95}H_{4,1}$ . Then this range is followed by a miscibility gap up to composition with higher content in silicon at around  $C_3FS_{1,52}H_{2,26}$ .

### 3.1.3 Determination of the full hydrated phase assemblage

The refined Rietveld control file was used to follow the evolution of the phase assemblage during the hydration of two BYF cements, A and B, giving the results shown in Figs 5 and 6. Cement B had a

lower ye'elimite and higher belite content than cement A, which led to more C-S-H formation at the expense of strätlingite. Cement A produces more strätlingite, which fixes a lot of water and so gives a significantly higher volume of solid phases (and thus a lower porosity) than cement B. For cement A, after hydration for one year, the volume of solids is around 2,2 times the reacted cement volume, which is similar than the ratio for a typical Portland cement. On the other hand, the ratio for cement B is only about 2,1. The difference is not only due to the consumption of strätlingite in cement B, however, it seems also at least partly due to a lower degree of belite hydration. Finally we may note that enough water is still available at 365 days for both cement A and B (roughly 70% of initial water consumed at 365 days for cement B).

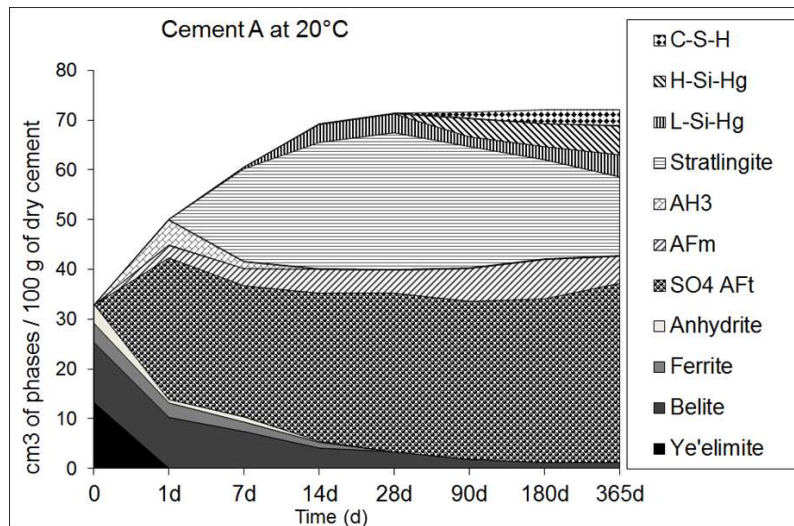


Figure 5 Phase assemblage (by volume) of cement A as a function of hydration time

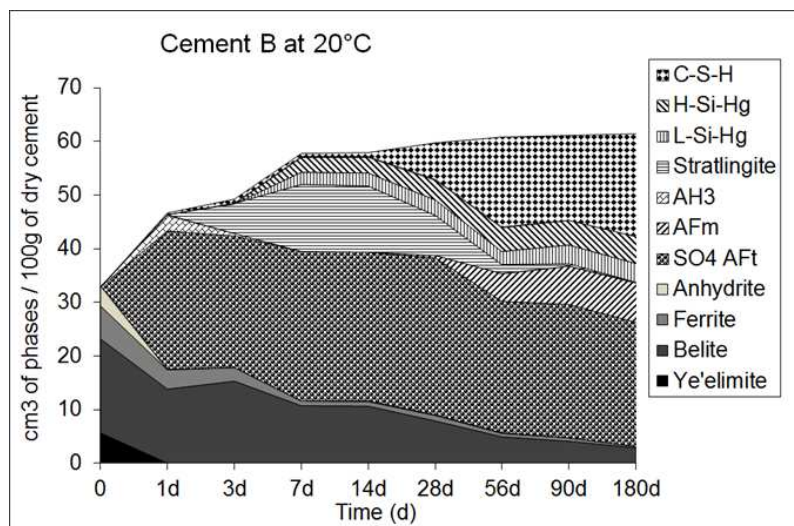


Figure 6 Phase assemblage (by volume) of cement B as a function of hydration time

### 3.2. Influence of calcium sulfate additions on the kinetics of belite hydration

Three different BYF cements were obtained by mixing 2.5% , 6.5% and 15.5% of ground anhydrite with ground clinker C, representing N values (the molar ratio of calcium sulfate over ye'elimite) of 0.4, 1, and 2.5, respectively. Table 6 gives the Rietveld-estimated relative masses of hydrated aluminate



phases for these cements hydrated at a water/cement ratio of 0.5 for 1 day. Note that at this hydration time the ye'elinite phase is fully hydrated in all three cements.

Table 6: Hydrated phase assemblages at 1 day (mass g / 100 g of initial cement)

	Hydrated phases		
	Ettringite	Calcium mono-sulfo-aluminate (sum of phases with 12 or 14H)	Aluminium hydroxide (AH <sub>3</sub> )
Cement C1	20	4	16
Cement C2	32	2	14
Cement C3	52	0	14

With increasing amounts of added anhydrite, the amount of ettringite increases and the amount of calcium mono-sulfo-aluminate decreases, in good agreement with the predictions of equations 3 and 4. The amount of aluminium hydroxide decreases only slightly, simply due to dilution of ye'elinite in the cements by added anhydrite. Interestingly, after 1 day, when the ye'elinite phase is fully hydrated, belite normally should start to hydrate but we can see in Fig. 7. that the onset of belite hydration is in fact increasingly delayed by increasing additions of calcium sulfate. Ongoing from 2.5% to 15.5% anhydrite addition, the onset of belite hydration is shifted from under 1 day to over 50 days.

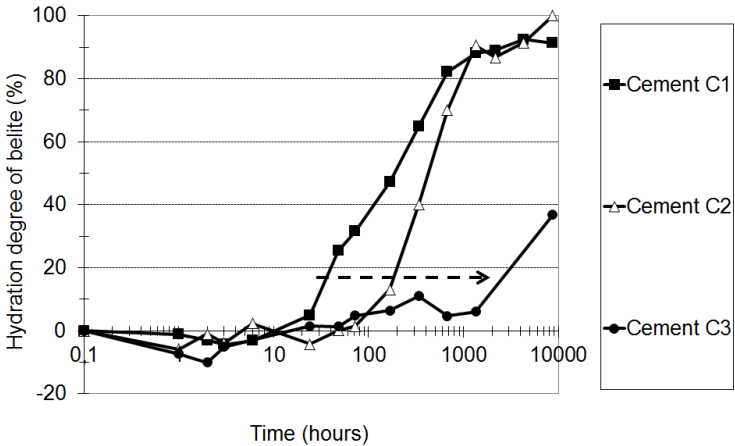


Figure 7 Hydration degree of belite vs. time for different anhydrite addition levels (with clinker C)

This delayed hydration of belite can have serious consequences on the rate of strength development, with the formation a “strength plateau” in which the strengths remains nearly constant for a significant time after the end of ye'elinite hydration (by about 1 day) until the onset of rapid belite hydration. To explain this phenomenon, our hypothesis is that ettringite precipitated at very early age forms a shell around cement grains that blocks water accessibility to belite surfaces (Zhang L. *et al.* 2002). Thus, the more ettringite formed initially, the more belite hydration will be delayed. Fig. 8 shows that the volume ratio between ettringite and cement paste at 1 day is about three times higher for cement C3 (with 15.5% anhydrite) than for cement C1 (with 2.5% anhydrite). Moreover, table 7 shows that at 1 day, the water consumption is about 50% for the cement with high amount of anhydrite (cement C3) compare to 35% for the cement with low level of anhydrite (cement C1).

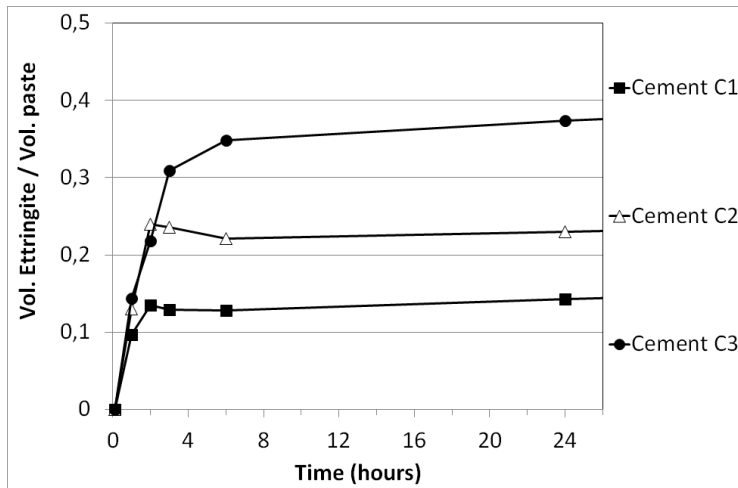


Figure 8 Volume ratio between ettringite and cement paste for different amount of calcium sulfate

Table 7 Water consumption and compressive strength at 1 day for cements with different anhydrite addition levels (with clinker C)

	Water consumption (% of initial water)	Compressive strength on standard mortar (MPa)
	At 1 day	At 1 day
Cement C1	35	16
Cement C2	38	19
Cement C3	50	23

Fig. 9. shows the microstructure of the cement paste with 6.5% of anhydrite (cement C2) at 1 day. We observe large areas of hydrates around clinker grains and especially belite grains. This layer of hydrates will limit water accessibility to cement surface and this mechanism will be amplified by the decreasing amount of the free water consumed during ettringite formation.

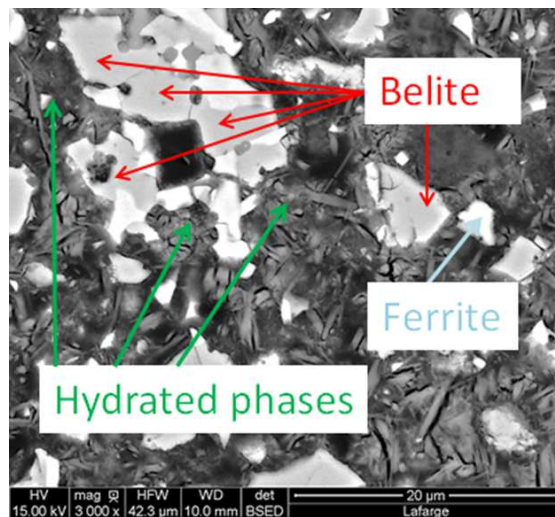


Figure 9 BYF cement paste microstructure at one day

So it appears that the control of ettringite formation by adjusting the added calcium sulfate level is a key lever for optimizing belite hydration and long-term strength development: by reducing the level of added calcium sulfate, it is possible to avoid the formation of the “plateau” in strength development that occurs between the end of ettringite formation and the onset of belite hydration. However, this optimum level of calcium sulfate for belite hydration may be modified with the water to cement ratio because a higher water content will give higher porosity and so better water accessibility to cement grains.

#### 4. Conclusions

We have developed a Rietveld control file that allows us to estimate the volume proportions of most of anhydrous and hydrated phases present in hydrated BYF cement pastes at all ages. This approach has allowed us to better understand the belite hydration kinetics, which is one of the more critical issues in dictating the performance of BYF cements. We have shown that belite hydration is delayed by excessive calcium sulfate additions, apparently because the high volume of ettringite formed at early ages blocks access to the surfaces of the un-hydrated belite crystals. Reducing the level of calcium sulfate addition leads to earlier belite hydration but at the same time reduces the 1 day strength. So we are faced with two opposing effects: on one hand we must add enough calcium sulfate to maximize ettringite formation from ye’elimite hydration) and on the other hand, the formation of ettringite will delay further cement hydration if its formation blocks belite surface. So in our opinion the control of ettringite formation is a key lever to optimize belite hydration and its resulting strength development. Progress in this area requires more research on the ideal clinker mineralogy for specific applications (optimal proportions of ye’elimite, belite and ferrite) and total binder compositions but also on chemical admixtures than can modify ettringite microstructure at early age.

#### Acknowledgements

Thomas Fuellmann from the Panalytical company is gratefully acknowledged for his advice and support in the development and improvement of our XRD procedures. We greatly also acknowledge Ellis Gartner for helpful discussions on these scientific topics.

#### References

- Chae W.H., Park D.C. and Choi S.H., 1996. Early hydration of modified belite cement prepared by adding borax, *The Korean Journal of Ceramics*, 2 (3), 147-151.
- Cuesta A., De la Torre A.G., Losilla E.R., Santacruz I. and Aranda M.A.G. 2014. Pseudocubic Crystal Structure and Phase Transition in Doped Ye’elimite, *Crystal growth & design*, 14, 5158-5163.
- Cuesta A., Alvarez-Pinazo G., Sanfelix S.G., Peral I., Aranda M.A.G. and De la Torre A.G., 2014. Hydration mechanisms of two polymorphs of synthetic ye’elimite, *Cement and Concrete Research*, 63, 127-136
- Dilnesa B.Z., 2011. Fe-containing hydrates and their fate during cement hydration: thermodynamic data and experimental study, *PhD thesis N°5262- EPFL*
- Gartner E. and Li G., 2006. World Patent Application WO2006/018569 A2
- Gartner E., 2004. Industrially interesting approaches to low CO<sub>2</sub> cements, *Cement and Concrete Research*, 34, 1489-1498.
- Gies A. and Knöfel D., 1986. Influences of alkalis on the composition of belite-rich cement clinkers and the technological properties of the resulting cement”, *Cement and Concrete Research*, 16 (3) , 411-422.
- Jelenic I., 1978. Hydration of B<sub>2</sub>O<sub>3</sub> stabilized  $\alpha'$  and  $\beta$  modifications of di-calcium silicate, *Cement and Concrete Research*, Vol 8, 173-180.
- Mehta P.K., 1980. Investigations on energy-savings cements, *World cement technology*, may, 166-177.
- Lea F.M., 1998. Lea’s chemistry of cement and concrete, chapter 9 low energy cement, *Edited by Peter C. Hewlett*

- Li G., Walenta G., and Gartner E.M., 2007. Formation and hydration of low-CO<sub>2</sub> cements based on belite, calcium sulfoaluminate and calcium aluminoferrite, *12<sup>th</sup> ICCC*, Montreal
- Morin V., Walenta G., Gartner E., Termkhajornkit P., Baco I. and Casabonne J.M., 2011. Hydration of a Belite-Calcium Sulfoaluminate-Ferrite cement : Aether<sup>TM</sup>, *13<sup>th</sup> ICCC*, Madrid.
- Suzuki K., 1980. Hydration and strength of  $\alpha$ ,  $\alpha'$  and  $\beta$ -di calcium silicates stabilized with Na-Al, K-Al, Na-Fe and K-Fe", *ICCC Paris*, Vol 2 , II-47-51.
- Wang Yanmou and Su Muzhen, 1993. The third series cement in China. *3<sup>rd</sup> Beijing International symposium*, 116-121
- Sharp J.H., Lawrence C.D. and Yang R., 1999. Calcium Sulfoaluminate cements – low energy cements, special cements or what?, *Advances in Cements Research*, 11, N°1, Jan, 3-13.
- Wang Jia, 2010. Hydration mechanism of cements based on low-CO<sub>2</sub> clinkers containing belite, ye'elimite and calcium alumino-ferrite, PhD thesis, Lafarge-universit  Lille.
- Wang Jia, Baco I., Morin V., Walenta G., Damidot D. and Gartner E., 2010. Hydration mechanism on cements based on low CO<sub>2</sub> clinker containing belite, ye'elimite and calcium alumino-ferrite. *7<sup>th</sup> ISCC*, Jinan, China
- Zhang L. and Glasser F.P., 2002. Hydration of calcium sulfoaluminate cement at less than 24 hours, *Cement and Concrete Research*, 14 , N°4, October, 141-155

---

<sup>i</sup> Corresponding author: [vincent.morin@lafarge.com](mailto:vincent.morin@lafarge.com), Tel +33-474 821 824, Fax ++33-474 168 0 00